Assessing the phenology of southern tropical Africa

Assessing the phenology of southern tropical Africa: a comparison of hemispherical photography, scatterometry and optical remote sensing

Casey M Ryan*, Mathew Williams, Timothy Hill, John Grace and Iain Woodhouse

School of GeoSciences, University of Edinburgh, Edinburgh EH9 3JN, UK.

* author for correspondence:

Tel: 0131 650 7722

Fax: 0131 662 0478

Email: casey.ryan@ed.ac.uk

Keywords

Phenology

Scatterometry

Enhanced vegetation index

Green up

Start of season

Land surface phenology

Canopy phenology

Abstract

The seasonal cycle of tree leaf display in the savannas and woodlands of the seasonally dry tropics is complex, and robust observations are required to illuminate the processes at play. Here we evaluate three types of data for this purpose, comparing scatterometry (QuikSCAT σ^0) and optical/NIR (MODIS EVI)) remotely sensed data against field observations in the woodlands of southern Africa. At a site in Mozambique, the seasonal cycles from both space-borne sensors are in close agreement with each other and estimates of plant area index estimates derived from hemispherical photography (correlation coefficients > 0.88). This agreement results in very similar estimates of the start of the growing season across different data types (range 13 days). Ku-band scatterometry may therefore be a useful complement to vegetation indices such as EVI for estimating the start of the growing season for trees in tropical woodlands. More broadly, across southern tropical Africa there is close agreement between scatterometry and EVI time series in woody ecosystems (>25% tree cover), but in areas of < 25% tree cover the two time series diverge and produce markedly different start of season dates (difference > 50 days). This is due to increases in σ^0 during the dry season, which were not matched by increase in EVI. The reasons for these increases are not obvious, but might relate to soil moisture, flowering, fruiting or grass dynamics. Further observations and modelling of this phenomenon is warranted to fully understand the causes of these dry season changes in σ^0. Finally, three different definitions of the start of season were examined, and found to produce only small differences in estimated dates, across all types of data.

Introduction

The timing of leaf display in tree species determines the duration of major fluxes of water, energy and carbon between the biosphere and atmosphere (Reich 1995; Chase *et al.* 1996; Baldocchi *et al.* 2005). In the seasonally dry tropics, trees are highly variable in their phenological behaviour, ranging from deciduous to briefly-deciduous to evergreen (Williams *et al.* 1997; de Bie *et al.* 1998; Singh and Kushwaha 2005). In the tropics, environmental control of leaf emergence is presumed to be related not to temperature (as in temperate and boreal regions), but neither is it simply related to patterns of precipitation and soil moisture (Myers *et al.* 1998; Borchert *et al.* 2002; Archibald and Scholes 2007; Higgins *et al.* 2011).

Improved understanding of tropical tree phenology is contingent upon accurate measurements of phenological behaviour. Such measurements can be ground-based, often involving the recording of a phenological event of interest in the canopy such as bud burst, or the collection of time series data such as carbon fluxes or leaf area index. Ground-based phenological data are however very sparse in many regions, particularly in tropical Africa (Schwartz 2003). A complementary approach is to use Earth observation (EO) data from satellites to record (bio)physical properties of the Earth surface that relate to phenological patterns of interest. Such measures of land surface phenology (LSP, (Liang and Schwartz 2009)), offer advantages in terms of regular and global data acquisition, but difficulties remain in linking LSP to ecologically relevant measure of canopy phenology (Studer *et al.* 2007; Doktor *et al.* 2009; Liang and Schwartz 2009; Liang *et al.* 2011).

Optical and infrared reflectances have been the workhorses of LSP studies to date (Liang and Schwartz 2009), often combined into a single "greenness' index such as NDVI (Normalised difference vegetation index) or EVI (enhanced vegetation index, (Huete *et al.* 2002)). However, such data acquisition is not without its difficulties: darkness, atmospheric composition, clouds and off-nadir viewing angle all reduce the availability of high quality, consistent measures of the land surface. Low or medium resolution active microwave remote sensing from scatterometry can also be used as source of LSP data and provides some relief from these constraints (Wagner *et al.* 1999; Woodhouse and Hoekman 2000b; Hardin and Jackson 2003; Frolking *et al.* 2006). It is however less widely used in monitoring vegetation phenology, and scatterometry LSP time series has not been widely related to ground-based canopy phenology data (Hardin and Jackson 2003). Ku-band scatterometry from the SeaWinds-on-QuikSCAT sensor has been shown to give comparable information to EVI in some vegetation types (Frolking *et al.* 2006), and to be useful for monitoring tropical grasslands (Hardin and Jackson 2003; Frolking *et al.* 2005). Ku-band wavelength (2.1 cm) is similar to many leaf lengths, and so a strong interaction between the microwave radiation and the leaves is expected (Ulaby *et al.* 1984) suggesting that these data could be a useful source of information on tree leaf phenology, and might provide a useful complement to optical LSP data. However, the two data sources respond to fundamentally different aspects of the land surface: scatterometry data are likely to respond to vegetation structure and moisture contents, as well being influenced by soil moisture, whereas EVI data will respond to chlorophyll content and amount of green leaf material.

A further issue in comparing LSP to canopy phenology is the method for extracting dates of phenological events from time series of LSP data (Reed *et al.* 1994; White *et al.* 2009; Schwartz and Hanes 2010). For instance, a common date of interest is the start of (growing) season date (SoS), the point at which tree leaf expansion starts. This date has been estimated from time series of LSP data in many ways, all of which are heuristic and have only limited relation to the biological event of interest, e.g. SoS is often defined as the point at which the EO quantity reaches half its annual maximum. The various definitions of SoS are often tangential to the canopy phenological processes of interest and the relationship between the two needs to be established empirically. In this study we evaluate this relationship between LSP and canopy phenology, and in particular how this relationship depends on both the type of LSP data (optical or scatterometry) and the definition of SoS. This is the first study to investigate the relationship between different SoS definitions derived from ground-based measurements, optical and microwave EO data.

Our study uses a detailed ground-based data set from a well-studied site in the woodlands of central Mozambique. We complement this with a regional study across all of southern tropical Africa, a region with complex climatology (Nicholson 2000), topography and vegetation (White 1983).

Key Questions

1. How does land surface phenology derived from different EO data types (optical and microwave) compare to ground-based estimates of canopy phenology?

2. In which ecosystems of southern tropical Africa are microwave-, and optical-derived phenologies congruent and what are the biophysical characteristics of areas where the two data sets diverge?
3. How similar are SoS dates derived from the different data types, and how is this affected by the specific way in which SoS is identified in the time series data?

Methods

Our methods consist of four components: 1) Collection of ground-based plant area index (PAI) data at a site in the woodlands of central Mozambique over 4 years; 2) processing of satellite LSP data at the Mozambique site and for all of southern tropical Africa over ten years; 3) analysis of the time series data including: cross correlation analysis; estimation of SoS dates based on different definitions; and 4) comparison of the regional EO phenologies to land cover and vegetation maps.

1) Data collection for Mozambique site

Site details

Fifteen square 1-ha permanent sample plots were installed in a range of woodland types in the Nhambita area of Gorongosa District, Sofala province, Mozambique in June 2004 (Ryan *et al.* 2011). The plots are spread across an area approximately 20 km by 30 km (centred on 18.979°S, 34.176°E), adjacent to the Gorongosa National Park (Tinley 1977). The vegetation on the plots included: (i) dry miombo woodland regrowing after clearance for agriculture; (ii) dry miombo degraded

by the removal of large stems for charcoal production; (iii) relatively undisturbed miombo in the National Park, both fenced and unfenced; and (iv) *Combretum* savanna on more hydromorphic soils (Mitchard *et al.* 2012; Ryan *et al.* 2012). The plots were randomly located along the track and road network in the area, and were all ≥ 250 m from a road or track. The location of the plots, on the western flank of the Rift Valley, means that they span a range of altitudes from 36-300 m, with corresponding changes in drainage and soil type.

Plant area index (PAI)

We monitored the seasonal cycle of plant area index (PAI) of trees using monthly hemispherical photography (Fuller 1999) for 48 months from June 2004 to May 2008 (inclusive) on the plots. On each plot, each month, we acquired nine images on a 20 x 20 m grid. Images were obtained under diffuse light conditions – either at dawn or dusk, or during overcast conditions – and from identical positions with the camera body oriented to the north and the lens rotated to the vertical. We used a Nikon Coolpix 4500 with a FC-E8 fisheye converter on a levelled tripod at 1.5 m height. The image is fully hemispheric. For logistical reasons we were unable to collect photos in seven months of the 48 month period of this study. A total of 4718 photos were acquired, coded with date and location and stored in a database (FileMaker Pro, Apple Computer Inc, CA). Each image was visually inspected and badly exposed or directly illuminated images were discarded (380 images). The images were then analysed to estimate PAI using the method of Ryan and Williams (2011).

Precipitation

Rain gauge data for the Nhambita study area were obtained from three sources: 1) daily rainfall totals from a manual rain gauge at the Gorongosa National Park headquarters at Chitengo, 25 km from the study site (Oct 2000-Nov 2005, provided by ARA CENTRO); 2) half hourly totals of rainfall from an automated weather station (Skye Instruments, UK) installed as part of this study adjacent to the Park gauge (Nov 2005-May 2008); 3) a manual gauge operated by Mr Piet van Zyl, at the centre of our study area. Data from 3) were used for a 4 month period (Nov 2007-Feb 2008) when the automatic gauge failed. For a five month period (November 2006-March 2007) when all three data sets are available, they show cumulative rainfall of 860, 860, and 878 mm, respectively. As these values are similar, we did not adjust the data from the different sources, and they were combined into one, daily resolution, time series.

2) EO land surface phenology data

Enhanced Vegetation Index (EVI)

Nine MODIS (Moderate Resolution Imaging Spectroradiometer) pixels of ground size 0.05° (~5.6 km) cover the 15 plots. Enhanced vegetation index (EVI) data (Huete *et al.* 2002) was obtained for these 9 pixels from both MODIS platforms, Terra and Aqua, and were provided as 16-day composites, 8 days out of synchrony with each other. The 0.05° resolution data is, although not the highest resolution available, suitable for extension to the regional scale analyses, and we extracted the full time series available at the time of processing (2000-2010). The 16-day composite product processes daily acquisitions using one of three compositing techniques (Huete *et al.* 2002) to minimise problems associated with clouds and off-nadir views.

We discarded all EVI data not flagged as 'good' or 'marginal' quality in the MODIS QA scheme and linearly interpolated over missing data values. The Terra and Aqua products were interleaved to create a time series of nominal 8 day resolution, although the real acquisition dates are a combination of dates from the higher resolution data. A smoothed time series was created using a second order Savitzky-Golay filter with a window of five data points. This relatively short window minimises the problem of shifting the time series as an artefact of the filtering.

Scatterometry data

Scatterometry data in the form of Ku-band normalised radar cross-section (σ^0) measurements from the SeaWinds instrument aboard QuikSCAT were obtained from the NASA Scatterometer Climate Record Pathfinder project (Long *et al.* 1993; Long 2010). The SeaWinds instrument makes dual polarization measurements of σ^0 at both vertical (VV, 54.1° nominal incidence angle) and horizontal (HH, 46°) polarizations using a conically scanning pencil-beam antenna. The Scatterometer Climate Record Pathfinder project provides enhanced resolution products, improving the relatively coarse scale (25km) of the original data using the Scatterometer Image Reconstruction (SIR) algorithm (Long *et al.* 1993; Spencer *et al.* 2000; Early and Long 2001). This method is based on utilising the frequent overpasses and wide swath to improve spatial resolution at the expense of temporal resolution, assuming no change in land surface properties over 4 days. The 4-day composite "egg" images were used, which have a nominal image pixel resolution of 4.45 km/pixel but an effective resolution of ~8-10 km in most areas. The images were interpolated to a 0.05° grid (~5.5 km) using Delaunay triangulation. Significant deviation from the "no change" assumption is expected to

occur only during the early part of the onset of the rainy season, where specific rain events will change the surface characteristics (in terms of soil moisture) over a short period of time. The impact will be added uncertainty when using data at highest resolution. The data smoothing applied within the SIR algorithm is expected to minimise the impact of this issue.

The σ^0 data had a different signal to noise ratio and a more consistent magnitude of high frequency variation, compared to the EVI data. A Savitzky-Golay filter with a 17 data point window removed the high frequency variations and again did not noticeably 'shift' the time series. Raw and smoothed data are shown in Fig 1. There were no missing σ^0 data.

Regional data

For the regional analysis we used the EO products described above, acquiring the full data sets for the area bounded by 2° to 26° S and 10° to 41° E. Regional rainfall data from the Tropical Rainfall Measuring Mission (TRMM, Kummerow *et al.* 1998) were acquired from the NASA Goddard Earth Sciences Data and Information Services Center. We used the 3B42 daily product which uses a combination of infra-red and microwave observations scaled to match monthly rain gauge analyses (Huffman *et al.* 2007). Data were obtained at 0.25° spatial resolution and linearly interpolated to 0.05°.

Vegetation types and tree cover

The regional phenology data were analysed by vegetation type based on the map of White (1983), which is based on pre-satellite era maps and expert interpretation and is thus independent of our EO data. We further analysed the regional phenology using

the 2005 MODIS vegetation continuous fields product (VCF, collection 4, version 3) (Hansen *et al.* 2003; Hansen *et al.* 2006). The 500 m product was reprojected and interpolated using a bicubic spline to match the 0.05° lat/long grid of the other datasets. We note that the tree cover data are not fully independent of the EVI time series data as some of the same reflectance data are used in the generation of the tree cover product, however the data used in the tree cover product only represent a small portion of the time series of EVI.

3) Analysis methods

Start of Season (SoS) definitions

We developed a set of definitions and related methods to convert time series of data into estimates of SoS. Many definitions and techniques have been used to derive LSP SoS from reflectance data (Reed *et al.* 1994; Kang *et al.* 2003; Zhang *et al.* 2003; Archibald and Scholes 2007; Bachoo and Archibald 2007; White *et al.* 2009), but with no consensus as to the optimum technique. The challenge is to avoid spuriously classing noise in the signal as SoS, whist detecting SoS as accurately as possible. Here we define the SoS as the time point where tree leaf bud break begins. For a given time series of phenology data, p, the SoS must postdate or equal the annual minimum of p, p_{min}, and of course, predate the following annual maximum. Many existing approaches define SoS as the mid point between annual minima and maxima (Higgins *et al.* 2011). However, here we are concerned with the *start* of the growing season, not some mid point. Two such definitions were found in the literature, the first (Zhang *et al.* 2003) is based on fitting logistic functions to phenological transitions, but these functions did not

yield useable fits to our data. The second, which did work effectively, utilised a backward-looking moving average (by Reed *et al.* (1994) modified by Archibald and Scholes (2007)). We term the resulting start of season date SoS_{AS}. To complement this definition, we developed two new ones: SoS_{LT} which looks for the start point of the first significant ($p>0.05$) positive linear trend in p and; SoS_{ON} which looks for the first 3 values of p to be significantly (2 SD of the noise) above the minimum. A full description of the three definitions is provided in Appendix 1. We also refer to p_{10}, which is 10% of the maximum of p for that growing season. This value provides a benchmark for assessing the reliability of SoS dates, and we assume that SoS should fall between p_{min} and p_{10}.

Estimates of start of season day-of-year (SoS) are subscripted with the SoS definition (one of $_{AS}$, $_{LT}$ or $_{ON}$ described above) and the source of the data used for the estimate, e.g. $SoS_{AS,PAI}$ indicates the SoS date from the backward-looking moving average derived from the PAI data, $SoS_{AS,EVI}$ for the SoS defined by the same method from the EVI data and $SoS_{AS,VV}$ and $SoS_{AS,HH}$ for the scatterometry data in each polarisation.

Comparison between ground data and EO data in Mozambique

To assess the congruence of the time series of EVI, PAI, σ^0_{HH}, and σ^0_{VV}, correlation coefficients were determined for the relationship of each time series against the other (denoted r). We also used cross correlation analysis to look for evidence of lags between the data series. SoS dates were derived for all the years when data were

available and compared between data sources (PAI, EVI, σ^0_{HH} and σ^0_{VV}) and the three SoS definitions (LT, AS, ON).

Results

Local observations

Based on the PAI, EVI and σ^0 data, leaf display on the Nhambita plots had a seasonal cycle with little inter-annual variability. PAI peaked in February/March and then fell to a minimum in September/October (Fig. 1) rising directly after the minimum in a brevi-deciduous manner. Small rain events were observed after October each year, with the main rains arriving from Oct 17- Dec 9.

The time series of PAI, σ^0 and EVI showed good agreement (Fig 1a b c) with significant correlations between each data source. PAI was best correlated to EVI (r = 0.94), and σ^0_{VV} (r = 0.90) followed by σ^0_{HH} (r = 0.88). The EO time series (EVI and σ^0) were also all very well correlated to each other (all r>0.95).

Judged by the cross-correlation coefficients, the seasonal cycle of PAI was shifted earlier that the LSP time series. σ^0_{VV} lagged PAI by 10 days, σ^0_{HH} lagged PAI by 15 days and EVI lagged PAI by 18 days. These lags should be viewed in the context of the monthly time step of the PAI data. The HH polarisation always returned a higher σ^0 than the VV (a difference of around 1.4 to 1.8 dB, which is expected due to the smaller incidence angle of the HH) and the HH:VV ratio varied with the seasonal cycle from 0.84 to 0.88, broadly in synchrony with leaf display.

Start of season in Nhambita (Table 1), based on PAI data and the LT definition ($SoS_{LT,PAI}$), occurred on similar dates each year: 25 Sept 2004, 21 Sept 2005, 6 Oct

2006 and 26 Sept 2007. The range of these dates is well within the one month resolution of the time series. It should be noted that in 2005, PAI data were missing near the SoS date. Mean SoS dates using the AS definition occurred 2 days later on average than with the LT definition (27 Sept±6 vs 29 Sept ±6 days). These SoS dates substantially preceded the point at which the time series reached 10% of its maximum each year ($p_{10,PAI}$ = 26 Oct ± 14).

Mean SoS estimates ranged over 28 days for all definitions and data sources (Table 1). Of the definitions, LT was generally the earliest, followed by AS and then ON. The scatterometry-derived SoS were always later than the EVI or PAI SoS dates. The range of SoS dates between definitions was slightly greater than the difference caused by the different data sources, and the relative difference caused by the data sources were consistent across SoS definitions. SoS dates derived from scatterometry were more variable between years than those from EVI, with PAI data giving the most consistent results.

Regional analysis

Looking across our regional study area and using $SoS_{EVI, AS}$ as an example, SoS arrived earliest in Angola and the Congo basin, spreading south and then east into Zambia, Botswana, Zimbabwe and Mozambique by day of year (DOY) 275 and arriving last on the east cost of Tanzania and Mozambique (DOY 300-350) (Figure 2).

The correlation between the two EO data types, EVI and σ^0 varied considerably across the study area but was high for most areas (Fig. 2): 76% of the study area showed $r > 0.8$ and 52% had $r>0.9$ (r is reported at zero lag). The HH polarised scatterometry

data were slightly better correlated to EVI than the VV, but both polarisations showed very similar patterns. For the remainder of the paper we discuss only the σ^0_{HH} results Locations with markedly low EVI vs σ^0_{HH} correlation are generally areas with seasonally inundated floodplains of large drainage systems such as the Zambezi, sparsely vegetated areas in the SW, and the equatorial forests of the Congo basin. The highest correlations were found in the woodland land cover types (Table 2) and in areas of intermediate tree cover (Fig. 5a). The sparsely wooded savannas in the SW of Botswana showed lower *r* compared to the more tree dominated systems to the north and east.

The strong correlations between scatterometry and EVI time series did not translate to similar SoS dates in many parts of the study area (Figure 4). Areas where SoS dates (mean of the three definitions) agreed well included most of the miombo woodlands and areas with moderate woody cover. In contrast, SoS dates diverged markedly in the south of the study area, including all of Botswana and most of Zimbabwe and the Zambezi valley. Vegetation types (Table 3) with a large difference in mean SoS_{EVI} compared to SoS_{HH} included Kalahari Acacia wooded grassland (mean difference -57 days [negative indicates SoS_{HH} is earlier), Undifferentiated woodland (-30), the transition between the two (-55) and Mopane woodland (-47). Dry miombo (-11) showed better agreement as did wet miombo (-5). No major vegetation types had SoS_{HH} later than SoS_{EVI}. Areas where the SoS differed between data types by > 10 days were restricted to areas with < 25% tree cover (Fig 5b). In areas with tree cover > 25%, SoS_{EVI} never differed from SoS_{HH} by more than 9 days.

Looking in more detail at the areas where SoS dates diverged markedly, the times series of EO data showed an anomalous pattern (Fig 6). σ^0 fell to a minimum at the start of the dry season but started increasing up to a month before the EVI and before any rainfall. This feature is widespread in Botswana and Zimbabwe and causes the much earlier SoS_{HH} values compared to SoS_{EVI}.

At the level of vegetation types, the three SoS definitions produce mean SoS dates that diverged by 5-12 days when using EVI data and 14-23 days using the scatterometry data (considering the 10 largest vegetation types). In the more wooded, northern part of the study area, the variability between SoS definitions exceeded the variability between data sources. However in the southern, sparse savanna areas, the previously noted large variation between EVI and σ^0. derived SoS dates greatly exceeded the variation between SoS definitions. The three SoS definitions produced more variable results using σ^0 compared to EVI.

The SoS dates fell within the range $p_{min} < SoS < p_{10}$ in >83% of pixel-years Table 2). No SoS dates were recorded prior to p_{min} for any SoS definition or data type. However, the ability to detect SoS prior to p_{10} varied considerable between definition and data type. Notably, the LT definition when used with EVI data, and the ON definition when used with scatterometry data failed to detect SoS prior to p_{10} in 11 and 17% of pixel-years (Table 1). The AS definition performed best, in that it reliably detected SoS after p_{min} and before p_{10}, with both data sources.

Discussion

1. How does land surface phenology derived from different EO data types

(optical and microwave) compare to ground-based estimates of canopy phenology?

Our results from a woodland site in Mozambique show that Ku-band scatterometry and EVI data record a land surface phenology (LSP) that is closely linked to the canopy phenology recorded by monthly hemispherical photos. Start of season (SoS) dates based on scatterometry data were on average 5-11 days later than those derived from hemispherical photos, depending on the definition of SoS, which given the monthly resolution of the ground data, suggests no substantive difference. The scatterometry LSP was also very similar to the EVI LSP, both in terms of SoS dates (2-11 days later, depending on SoS definition) and the correlation between time series (r>0.94).

The close agreement between σ^0 of both polarisations and EVI is expected to be due to several processes (Hardin and Jackson 2003), including increased soil moisture and green vegetation in the wet season. The green vegetation includes both grass and tree canopy elements, and is important due to its higher dielectric constant compared to dry vegetation (therefore increasing volume scattering), and the seasonal dynamics of chlorophyll content, growth and die-back (which influence both volume scattering and EVI). Soil moisture is the trigger of grass growth, which leads to greater leaf display (and hence EVI), and also increases surface scattering, which increases σ^0 (Woodhouse and Hoekman 2000a; Frolking *et al.* 2011).

To our knowledge, no previous studies have compared ground-based tree canopy observations to scatterometry LSP in mixed tree-grass ecosystems. However, at several grassland sites in South America, Hardin and Jackson (2003) concluded that

changes in σ^0_{HH} and σ^0_{VV} were largely a function of grass biomass or LAI and Frolking *et al.* (2005) showed that interannual variability in grass biomass in the USA was related to variability in Ku-band scatterometry. As the Mozambique site has a substantial grass understory (Ryan 2009), grass dynamics are likely contributing to seasonal variations in σ^0 in our study. However, prior to the commencement of the rains, increases in σ^0, EVI, and PAI are observed (Fig 1). Grass biomass cannot develop before the start of the rainy season (Chidumayo 2001; Hoffmann *et al.* 2005; Archibald and Scholes 2007), but in contrast tree leaf expansion can start weeks or months before the rains (Frost 1996; de Bie *et al.* 1998; Devineau 1999; Chidumayo 2001; Simioni *et al.* 2004; Do *et al.* 2005 ; Archibald and Scholes 2007; Higgins *et al.* 2011). Changes in σ^0 of ~2 dB are observed prior to the onset of the rainy season, suggesting that, in wooded areas, tree canopy phenology drives most of the change in σ^0, a conclusion that is supported by modelling studies (Ulaby *et al.* 1984). These observations, coupled with the close correlation between PAI (which records only tree phenology, not grass) and σ^0 time series suggest that σ^0 is responding to the development of the tree canopy, perhaps with a further contribution from the grass. Ku-band scatterometry may therefore be useful in determining the start of the growing season for trees in miombo woodland ecosystems.

Hardin and Jackson (2003) also found that σ^0_{HH} was more sensitive to soil moisture than σ^0_{VV}, resulting in a relationship between the difference, $\sigma^0_{HH} - \sigma^0_{VV}$, and rainfall/soil moisture. We have not standardised the two polarisations to a similar incidence angle, but still see a seasonal variation in the difference that is linked to the pattern of dry and wet seasons, with particularly high values in very intense rainy

seasons (2005 and 2007, Fig 1). However the magnitude of this variation is small (~0.2 dB) and variations are observed outwith the rainy season (e.g. Aug 05, Aug 07 in Fig 1).

2. *In which ecosystems of southern tropical Africa are microwave - and optical-derived phenologies congruent and what are the characteristics of areas where the two data types diverge?*

In line with the findings at the Mozambique site, the scatterometry and EVI data were very well correlated (r^2 >0.8), and produced similar SoS dates, across the miombo woodlands and in regions with >25% tree cover. Previous studies have observed a close link (r^2 >0.57) between MODIS-estimated LAI and σ^0 in some deciduous broadleaf forests in North America, savannas in Benin and Sudan, shrublands in Botswana and grasslands in N America (Frolking *et al.* 2006). We find similar or stronger correlations between EVI and σ^0 in much of Southern Tropical Africa, including all woodlands, dry forests, sparse savannas and grasslands. Areas where EVI and σ^0 are not significantly correlated included seasonally inundated grasslands and areas with little seasonality (deserts and rain forests). However, in the areas that do exhibit a strong correlation, it is clear that *r* provides only a crude measure of the similarity of the LSP signals and when SoS dates were extracted, a much more complicated picture emerges.

Firstly, even in areas with very high correlation (r>0.91), scatterometry-derived SoS was often earlier than EVI-derived SoS: by one week in wet miombo and two weeks in dry miombo (Table 3). This may reflect the fact that new miombo leaves are not normally green and new leaves increase in chlorophyll content for up to several weeks after bud burst (Tuohy and Choinski 1990; Choinski and Johnson 1993). Thus the EVI may be lower for a given leaf area than later in the season. The structural and

420 moisture-related information provided by the scatterometry may thus be decoupled from the biochemical information in the EVI reflectance data. However it may also be that the signal-to-noise ratio and temporal resolution of the σ^0 data are better suited to earlier detection of SoS. In particular, the more frequent observations of σ^0 make the linear trend method more powerful and may enable significant trends to be detected earlier compared to the quasi 8-day intervals between the MODIS products used here.

Secondly, the more moderate strength of correlation ($0.65 < r < 0.88$) in areas of sparse savanna (tree cover < 25%) in the south of the study area (e.g. Mopane, Acacia savanna and transition woodlands) belies major discrepancies in LSP during the dry season and the start of the growing season (Figs 4 & 6). These discrepancies result in
430 very large (20-47 days) differences in SoS dates derived from the two sources of LSP data (Fig 4). The divergence of σ^0 and EVI in areas of sparse woody cover is interesting and we now speculate on what could cause the observed transient increase in σ^0 prior to the rains (Fig 6). Increases in soil moisture can probably be ruled out as there is no rainfall recorded during the divergence event (and, although TRMM data may miss small rain events, we have found that in Nhambita TRMM overestimates early season rainfall compared to ground observations, data not shown). However as the soil dries out, the increased depth of penetration of the radar energy may allow it to interact with previously 'hidden' features, such as roots and impermeable pans, which may cause an increase in backscatter via surface scattering. Changes to the soil surface, perhaps due to
440 cracking or fire might play a role, but it is difficult to envisage how these effects could be transient within the dry season. The senescence, structural changes, and changing moisture content of the substantial grass layer in these systems may well play a strong

role in altering σ^0 (see above) and deserves further study. It is also possible that dry season fruiting or flowering in the tree canopy could increase σ^0 in the transient manner observed, although whether the magnitude of this effect would corresponding to the ~ 0.5 dB changes observed is questionable. Until this issue is understood, scatterometry-derived LSP cannot be easily related to canopy phenology or other ecological phenomena with confidence in savannas with < 25% tree cover.

3. *How similar are SoS dates derived from the different data types, and how is this affected by the definition of SoS?*

The three SoS definitions produced more variable results using σ^0 compared to EVI. The range between the three SoS definitions was between 1 and 9 days when using EVI data and 15-19 days using the scatterometry data (considering the 10 most extensive vegetation types). In the northern part of the study area in the woodlands, the variability between SoS definitions exceeded the variability between data sources. However in the southern, sparse savanna areas, the previously noted large variation between EVI and σ^0-derived SoS dates greatly exceeded the variation between SoS definitions.

None of the SoS definitions produced SoS dates prior to p_{min}, but their ability to detect SoS before 10% of the season's maximum (p_{10}) varied both by definitions and data sources (Table 1). The LT definition, when used with EVI data, failed to detect SoS before p_{10} in 11% of pixel-years, whereas when used with scatterometry data, it only failed in this regard 5 % of the time, probably due to the power of more frequent observations. Conversely, the ON definition failed to detect SoS prior to p_{10} in 17-20%

of pixel-years when used with the scatterometry data, but this was reduced to 1% when used with EVI data. This can probably be attributed to the poorer signal to noise ratio of the scatterometry data. The AS method was successful in detecting SoS prior to p_{10} in > 95% of pixel-years, regardless of data type, and is thus probably the most suitable for use with both data types, whereas the other methods were less useful with one or other of the data types. The AS method also produced intermediate SoS dates, later than LT but prior to ON.

Conclusions

- At a woodland site in central Mozambique, ground based plant area index measurements recorded a seasonal cycle of leaf display similar to that observed from scatterometry and optical remote sensing. Correlations between the data sources were strong (r>0.94), and start of season dates extracted from the time series were similar (mean difference < 11 days).
- At a regional scale, the good agreement between QuikSCAT σ^0 and MODIS EVI was found to extend across the woodlands of southern tropical Africa. In areas with tree cover > 25%, start of season dates estimated with EVI and scatterometry data never differed by > 9 days, suggesting that scatterometry data and EVI are both useful tools for assessing the land surface phenology in African woodland ecosystems.
- In more sparsely wooded ecosystems (<25% tree cover) such as the Acacia woodlands and mopane, the σ^0 and EVI time series diverged, with increases in σ^0 in the dry season, months prior to EVI increases or TRMM-recorded rainfall. This anomalous σ^0 increase resulted in much earlier start of season dates being recorded

from scatterometry data in comparison to EVI data (>30 days). Possible reasons for this difference include variations in soil moisture or soil roughness, the occurrence of tree flowering and fruiting, or grass dynamics. Further investigation of this phenomenon using ground-based observations and process-based modelling is warranted to fully understand the causes of these dry season changes in σ^0.

- Three different definitions of the start of season produced only modest differences in estimated start of season dates (<19 days), and produced similar results with both EVI and σ^0 data. A backwards-looking running average method worked best with both σ^0 and EVI data, in that it most often produced start of season dates between the minimum and 10% of each growing season's maximum value of the time series.

Acknowledgements

We gratefully acknowledge the NASA Scatterometer Climate Record Pathfinder project (www.scp.byu.edu), which provided the Resolution-enhanced SeaWinds backscatter data. Thanks to Meg Coates Palgrave for helpful comments and Tristan Quaife (NCEO and University of Exeter), Rob Clement, and Sophie Bertin (University of Edinburgh) for useful discussions. Fieldwork assistance from the following made this work possible: Envirotrade Ltd and the Nhambita community, including Piet van Zyl, Antonio Serra, Albasino 'Joe' Mucavel, Alphonso Journal, Romaio Saimone, Salomaõ 'Baba' Nhangue. Special thanks to Joanne Pennie and Gary Goss.

Appendix 1: definitions of start of season

Green up detection definitions

All data were analysed on a per-pixel basis and in separate year-long sections starting from May 1. Each time series were normalised to a range of 0 -1 to avoid the influence of the amplitude of the time series in different ecosystems. Both raw and smoothed data (described in the main text) were used. p_{min} and p_{10} were estimated from the smoothed time series. For robustness, p_{10} was defined as 10% of the 95% percentile of the data for that year.

1. Backwards looking running average (SoS_{AS})

Archibald and Scholes (2007) defined the SoS as occurring at measurement *i*, when:

$$p_i > \overline{p_{i-1\ldots i-4}}$$

where p_i is the EO quantity for measurement at time *I* and $\overline{p_{i-1\ldots i-4}}$ is the mean of the EO quantity of the past four observations.

2. Linear Trend (SoS_{LT}).

The LT definition looks for the data point at which there is a significant, positive slope to the following values of *p* over two time periods. It fits (using linear least squares) two lines, starting at timepoint *i* and using all data points for the following t_{short} and t_{long} periods (default values 30 and 60 days, respectively). The slopes, s_{short} and s_{long}, of the lines and the probabilities (P_{short} and P_{long}) of obtaining a correlation as large as the

observed value by random chance were estimated using the *polyfit* and *corrcoef* functions of Matlab. SoS_{LT} is indicated by all of the following being true:

$s_{short} > 0$, $s_{long} > 0$, $P_{short} < P_{crit}$, $P_{long} < P_{crit}$.

Where the default value of P_{crit} is 0.05. In addition, an extra constraint was added to ensure that local minima were avoided. Thus, the following must also be true:

$p_i < p_{i+1} < p_{i+2}$

3. Out of the noise (SoS_{ON}).

This method estimates the noise (N) in the signal as the difference between the smoothed data (p) and the observed raw data (p^*). It then defines SoS as the first point after p_{min} when n consecutive values (default $n = 3$) of p exceed $p_{min}+N$. SoS_{ON} occurs at timepoint $_i$, when all of the following are true:

$p^*_i > p_{min}+N$,

$p^*_{i+1} > p_{min}+N$,

…

$p^*_{i+n} > p_{min}+N$,

Where, $N = 1.98 \cdot \sqrt{\frac{\sum([p_i - p_i^*] - \overline{[p-p^*]})^2}{n-1}}$ and n is the number of observations in the annual time series of raw data p^* and smoothed data p.

Tables

Table 1. Start of Season day-of-year (mean ±SD of 4 years) for a site in the miombo woodlands of Mozambique, estimated from both ground based hemispherical photos (PAI) and space borne optical/NIR data (EVI) and scatterometry data in two polarisations (σ^0_{VV} and σ^0_{HH}). Three different definitions of SoS are used, one based on the start point of a linear positive trend in the time series (LT), a backward looking moving average (AS), another based on the first significant difference from the minimum (ON).

Data source	SoS definition		
	LT	**AS**	**ON**
PAI	271±6	273±6	
EVI	267±8	283±12	282±10
σ^0_{VV}	277±17	285±17	295±14
σ^0_{HH}	276±19	284±17	293±14

Table 2. Percentage of pixel-years when Start of Season (SoS) was detected prior to the time series reaching 10% of its yearly maximum (p_{10}). Three different definitions of SoS are used, one based on the start point of a linear positive gradient in the time series (LT), a backward looking moving average (AS), another based on the first significant difference from the minimum (ON).

Data source	**SoS definition**		
	LT	**AS**	**ON**
EVI	11%	5%	1%
σ^0_{HH}	5%	2%	20%
σ^0_{VV}	4%	2%	17%

Table 3. Summary of phenological characteristics of the major vegetation types of southern tropical Africa. The ten largest vegetation types are presented, which occupy 76% of the land area of the study region.

Vegetation type	Area (% of study area)	Mean Start of Season date						Correlation (r) between EVI and σ^0 timeseries		% tree cover from MODIS VCF
		EVI data			Scatterometry (HH) data					
		LT	AS	ON	LT	AS	ON	VV-pol	HH-pol	
Wetter Zambezian miombo woodland	20%	240	248	249	233	237	249	0.91	0.91	35
Drier Zambezian miombo woodland	11%	278	279	282	259	263	275	0.91	0.91	24
Mosaic of lowland rain forest & secondary grassland	9%	229	237	236	228	235	244	0.69	0.73	36
Colophospermum mopane woodland & scrub woodland	8%	285	283	289	226	235	242	0.78	0.79	12
Undifferentiated woodland	6%	273	273	279	232	240	252	0.86	0.86	19
Kalahari Acacia wooded grassland & deciduous bushland	5%	276	271	279	204	212	222	0.77	0.80	2
East African coastal mosaic	5%	293	297	295	296	304	311	0.89	0.90	28
Transition from undifferentiated woodland to Acacia deciduous bushland & wooded grassland.	5%	278	275	283	212	216	227	0.78	0.81	5
Guineo-Congolian rain forest: drier types	4%	246	258	254	258	264	274	0.31	0.30	51
Mosaic of dry deciduous forest & secondary grassland	4%	264	268	272	226	228	244	0.89	0.90	15

Figures

Figure 1. Phenology of the woodland of Nhambita, Mozambique. A) Plant area index of the tree canopy derived from 14 permanent sample plots. Crosses show the full range of dates over which each observation was obtained and the mean ± 1 standard error of the PAI of the 14 plots. The line shows a smoothed fit using a cubic spline. B) MODIS EVI for the nine 0.05° pixels that cover the plots. The crosses show the time span over which each observation is composited and the standard error of the mean of the nine pixels. C) QuikSCAT σ^0 for the nine pixels that cover the study area. Each 4-day observation is marked with a symbol. The lines show a filtered time series using a Savitzky-Golay filter with a 21 day window. D) as C) but for the difference between HH and VV polarisations. Two smoothed lines are shown, one (thin) with a 21 day window, the other (thick) with a 31 day window. E) daily rainfall from a local rainguage.

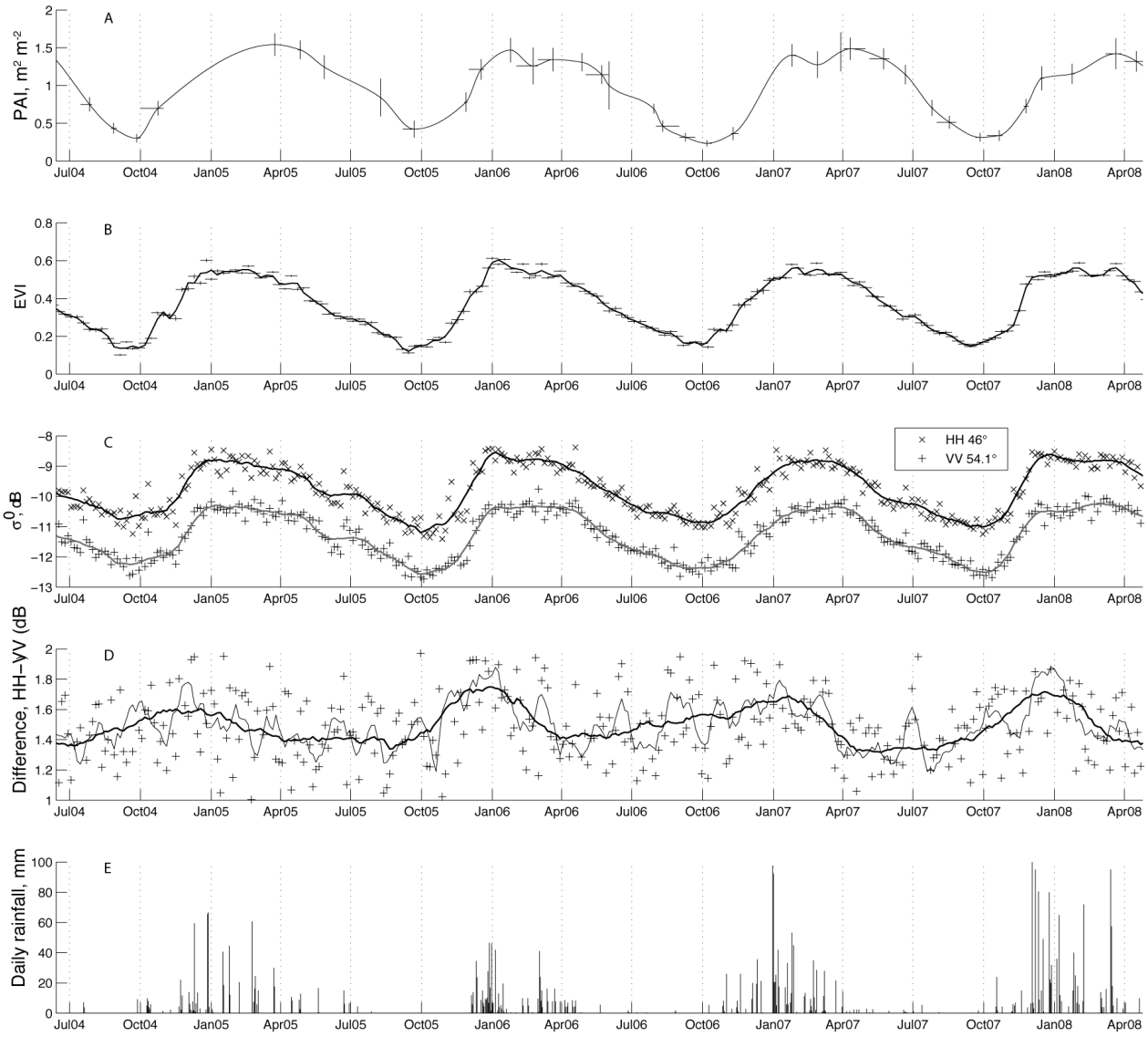

590

Figure 2. Map of Start of Season based on EVI data and using the using the linear trend definition of SoS. Areas where no SoS could be estimated are shown in grey.

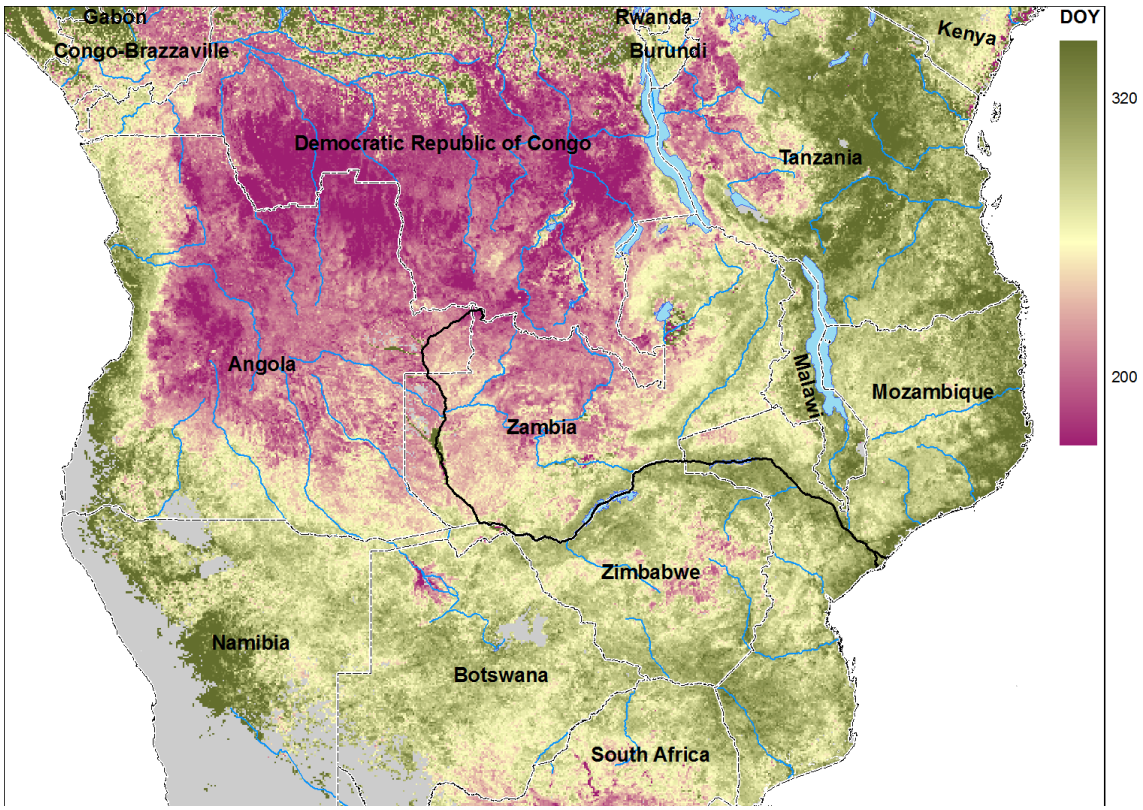

Figure 2. Map of agreement between the EVI and scatterometry (σ^0_{HH}) time series. The square of the correlation coefficient (r^2) between the two time series is shown. The Zambezi River is marked with a thick black line, and the areas of inundated grassland defined by the WWF eco-regions map (Olson *et al.* 2001) are marked with a dashed black line.

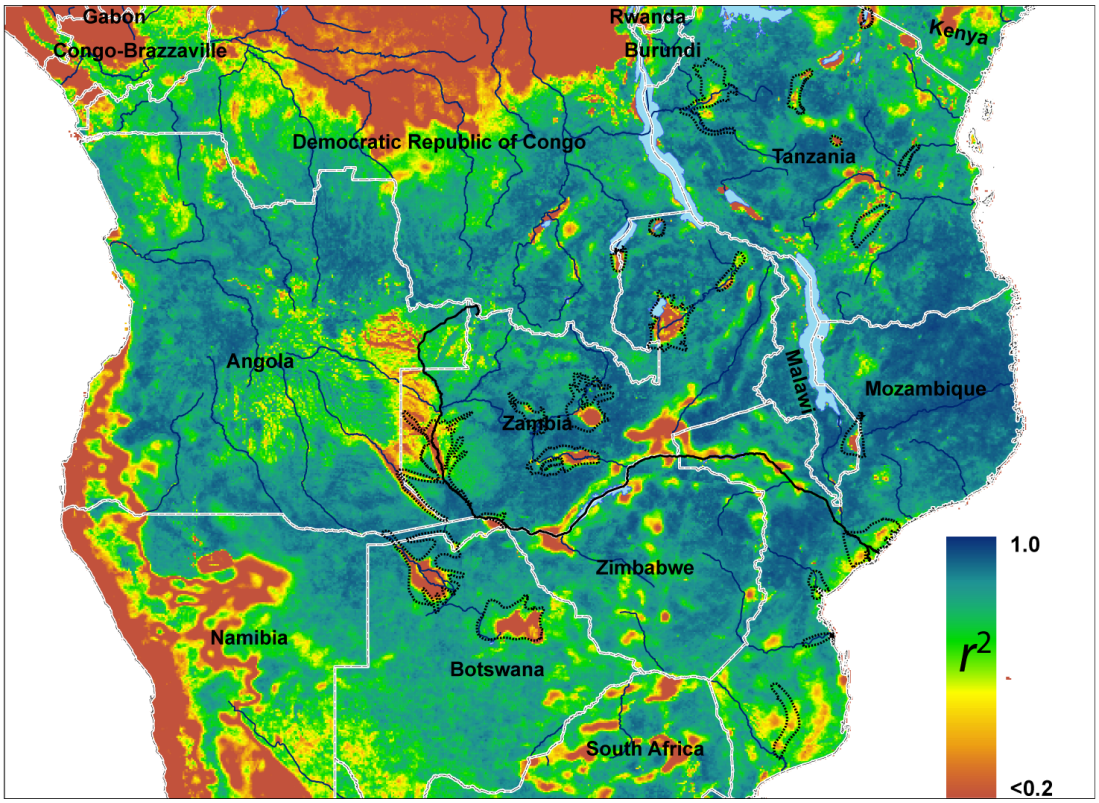

Figure 4. Difference between SoS dates derived from EVI and scatterometry data (σ^0_{HH}). Blue shows areas where start of season (SoS) dates estimated with scatterometry data are earlier than EVI-derived SoS. In these areas, the seasonal cycle of vegetation 'greenness', recorded by the EVI, diverges from the seasonal cycle of biophysical properties of the land surface recorded by the scatterometry data. The reasons for this are unclear (see discussion). SoS dates are the mean of 10 years and the three definitions of SoS.

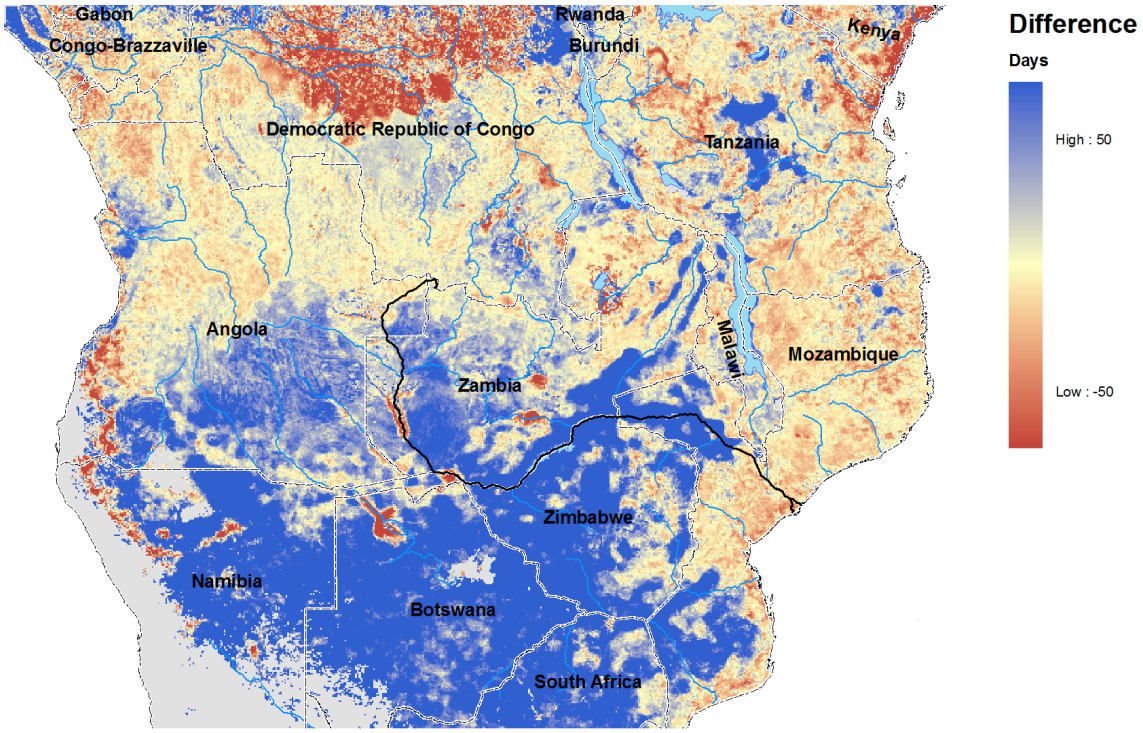

Figure 5a. The strength of the relationship between the EVI and backscatter time series. Each bar shows the mean correlation coefficient (*r*) between the two data sources as a function of tree cover for all pixels in the tree cover bins.

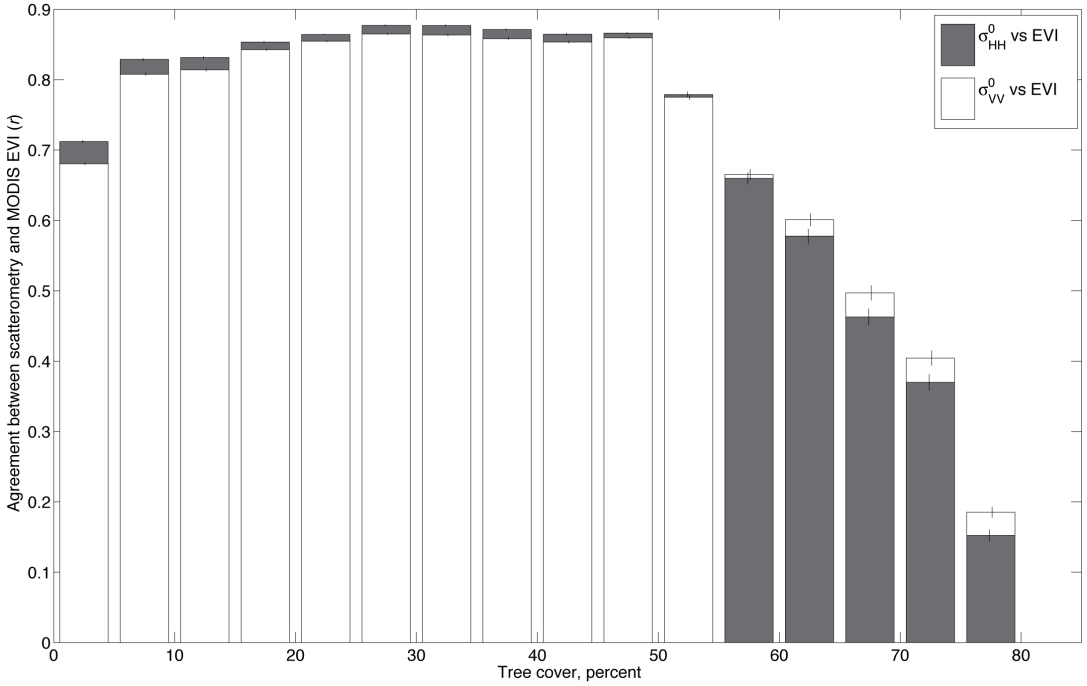

Figure 5b. The difference between scatterometry- and EVI-derived start of season dates, as a function of tree cover. Tree cover data is from the MODIS VCF product.

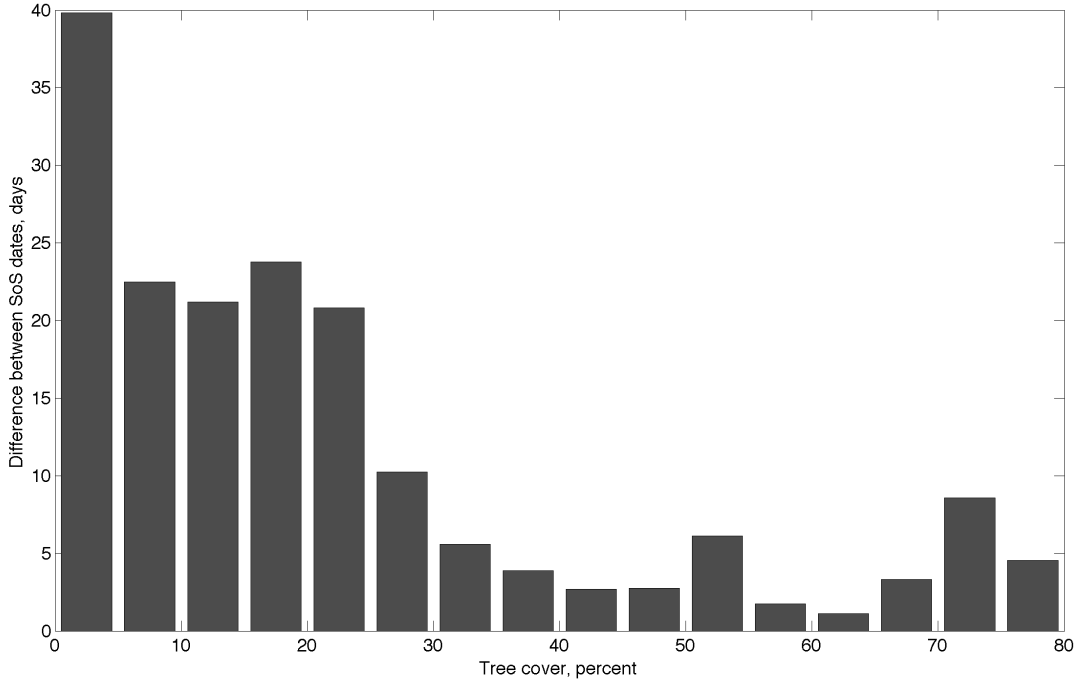

Figure 6. Time series of EVI and σ^0 for two example locations in sparsely wooded southern Africa. Note the excursion of σ^0 in the late dry season, whilst EVI is declining and prior to rainfall. Such excursions result in large differences between start of season dates derived from the two data sets.

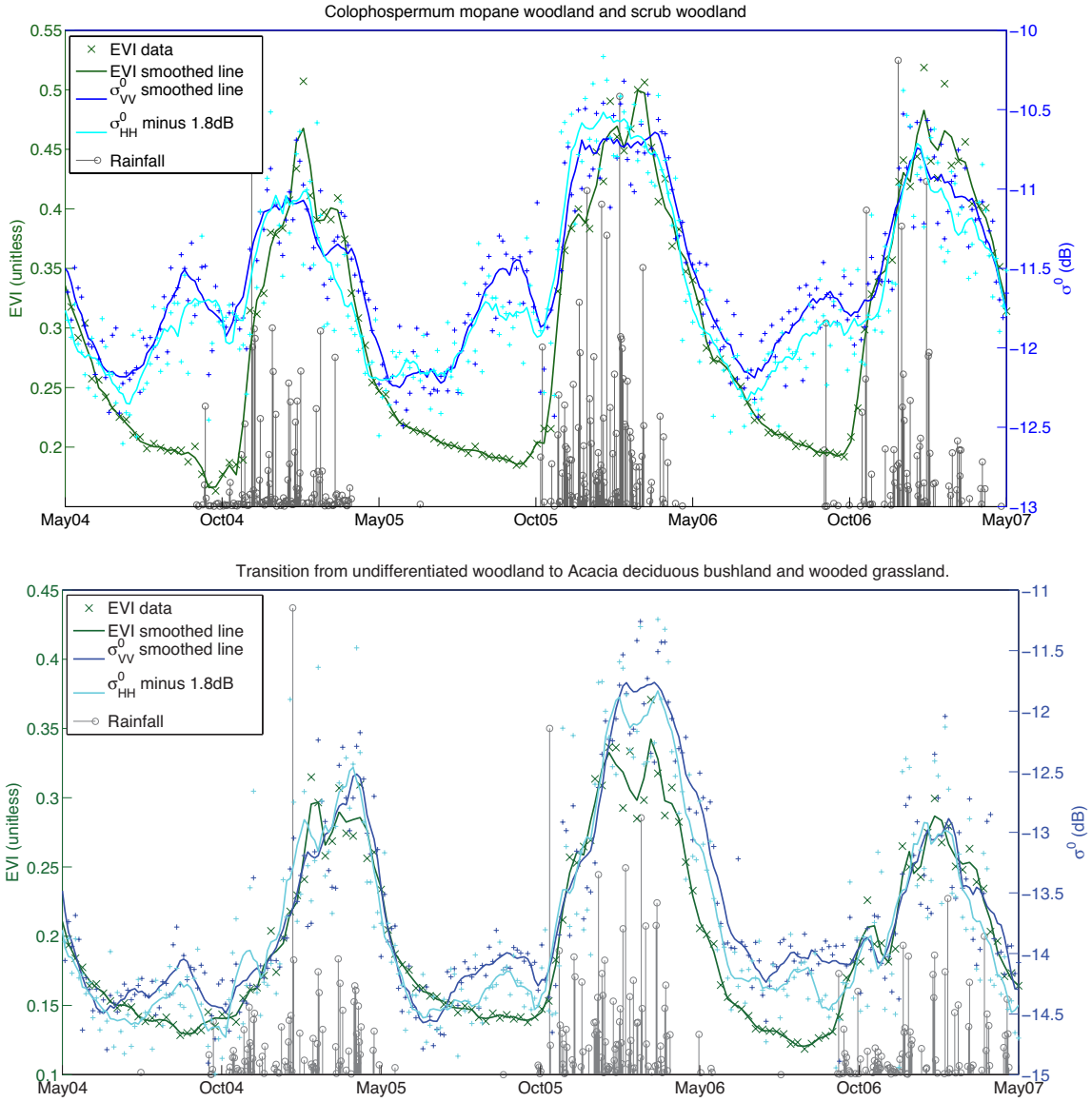

630

References

Archibald, S. and R. J. Scholes (2007). "Leaf green-up in a semi-arid African savanna separating tree and grass responses to environmental cues." Journal of Vegetation Science **18**: 583-594.

Bachoo, A. and S. Archibald (2007). Influence of Using Date-Specific Values when Extracting Phenological Metrics from 8-day Composite NDVI Data. MultiTemp 2007: International Workshop on the Analysis of Multi-temporal Remote Sensing Images.

Baldocchi, D. D., T. A. Black, P. S. Curtis, E. Falge, J. D. Fuentes, A. Granier, L. Gu, A. Knohl, K. Pilegaard, H. P. Schmid, R. Valentini, K. Wilson, S. Wofsy, L. Xu and S. Yamamoto (2005). "Predicting the onset of net carbon uptake by deciduous forests with soil temperature and climate data: a synthesis of FLUXNET data." International Journal of Biometeorology **49**(6): 377-387.

Borchert, R., G. Rivera and W. Hagnauer (2002). "Modification of vegetative phenology in a tropical semi-deciduous forest by abnormal drought and rain." Biotropica **34**(1): 27-39.

Chase, T. N., R. A. Pielke, T. G. F. Kittel, R. Nemani and S. W. Running (1996). "Sensitivity of a general circulation model to global changes in leaf area index." J. Geophys. Res. **101**(D3): 7393-7408.

Chidumayo, E. N. (2001). "Climate and phenology of savanna vegetation in southern Africa." Journal of Vegetation Science **12**(3): 347-354.

Choinski, J. S. and J. M. Johnson (1993). "Changes in Photosynthesis and Water Status of Developing Leaves of Brachystegia-Spiciformis Benth." Tree Physiology **13**(1): 17-27.

de Bie, S., P. Ketner, M. Paasse and C. Geerling (1998). "Woody plant phenology in the West Africa savanna." Journal of Biogeography **25**(5): 883-900.

Devineau, J. L. (1999). "Seasonal rhythms and phenological plasticity of savanna woody species in a fallow farming system (south-west Burkina Faso)." Journal of Tropical Ecology **15**: 497-513.

Do, F. C., V. A. Goudiaby, O. Gimenez, A. L. Diagne, M. Diouf, A. Rocheteau and L. E. Akpo (2005). "Environmental influence on canopy phenology in the dry tropics." Forest Ecology and Management **215**(1-3): 319-328.

Doktor, D., A. Bondeau, D. Koslowski and F.-W. Badeck (2009). "Influence of heterogeneous landscapes on computed green-up dates based on daily AVHRR NDVI observations." Remote Sensing of Environment **113**(12): 2618-2632.

Early, D. S. and D. G. Long (2001). "Image reconstruction and enhanced resolution imaging from irregular samples." Geoscience and Remote Sensing, IEEE Transactions on **39**(2): 291-302.

Frolking, S., M. Fahnestock, T. Milliman, K. McDonald and J. Kimball (2005). "Interannual variability in North American grassland biomass/productivity detected by SeaWinds scatterometer backscatter." Geophys. Res. Lett. **32**(21): L21409.

Frolking, S., T. Milliman, K. McDonald, J. Kimball, M. Zhao and M. Fahnestock (2006). "Evaluation of the SeaWinds scatterometer for regional monitoring of vegetation phenology." J. Geophys. Res. **111**(D17): D17302.

Frolking, S., T. Milliman, M. Palace, D. Wisser, R. Lammers and M. Fahnestock (2011). "Tropical forest backscatter anomaly evident in SeaWinds scatterometer morning overpass data during 2005 drought in Amazonia." Remote Sensing of Environment **115**(3): 897-907.

Frost, P. (1996). The ecology of Miombo woodlands. The Miombo in transition : woodlands and welfare in Africa. B. M. Campbell. Bogor, Indonesia, Center for International Forestry Research: 11-55.

Fuller, D. O. (1999). "Canopy phenology of some mopane and miombo woodlands in eastern Zambia." Global Ecology and Biogeography **8**(3-4): 199-209.

Hansen, M., R. DeFries, J. R. Townshend, M. Carroll, C. Dimiceli and R. Sohlberg (2006). Vegetation Continuous Fields MOD44B, 2005 Percent Tree Cover. C. P. University of Maryland, Maryland.

Hansen, M. C., R. S. DeFries, J. R. G. Townshend, M. Carroll, C. Dimiceli and R. A. Sohlberg (2003). "Global Percent Tree Cover at a Spatial Resolution of 500 Meters: First Results of the MODIS Vegetation Continuous Fields Algorithm." Earth Interactions **7**(10): 1-15.

Hardin, P. J. and M. W. Jackson (2003). "Investigating SeaWinds terrestrial backscatter: Equatorial savannas of South America." Photogrammetric Engineering and Remote Sensing **69**(11): 1243-1254.

Higgins, S. I., M. D. Delgado-Cartay, E. C. February and H. J. Combrink (2011). "Is there a temporal niche separation in the leaf phenology of savanna trees and grasses?" Journal Of Biogeography **38**(11): 2165-2175.

Hoffmann, W. A., E. R. da Silva, G. C. Machado, S. J. Bucci, F. G. Scholz, G. Goldstein and F. C. Meinzer (2005). "Seasonal leaf dynamics across a tree density gradient in a Brazilian savanna." Oecologia **145**(2): 307-316.

Huete, A., K. Didan, T. Miura, E. P. Rodriguez, X. Gao and L. G. Ferreira (2002). "Overview of the radiometric and biophysical performance of the MODIS vegetation indices." Remote Sensing of Environment **83**: 195-213.

Huffman, G. J., R. F. Adler, D. T. Bolvin, G. Gu, E. J. Nelkin, K. P. Bowman, Y. Hong, E. F. Stocker and D. B. Wolff (2007). "The TRMM Multisatellite Precipitation Analysis (TMPA): Quasi-Global, Multiyear, Combined-Sensor Precipitation Estimates at Fine Scales." Journal of Hydrometeorology **8**(1): 38-55.

Kang, S., S. W. Running, J. H. Lim, M. Zhao, C. R. Park and R. Loehman (2003). "A regional phenology model for detecting onset of greenness in temperate mixed forests, Korea: an application of MODIS leaf area index." Remote Sensing of Environment **86**: 232-242.

Kummerow, C., W. Barnes, T. Kozu, J. Shiue and J. Simpson (1998). "The Tropical Rainfall Measuring Mission (TRMM) Sensor Package." Journal of Atmospheric and Oceanic Technology **15**(3): 809-817.

Liang, L. and M. Schwartz (2009). "Landscape phenology: an integrative approach to seasonal vegetation dynamics." Landscape Ecology **24**(4): 465-472.

Liang, L., M. D. Schwartz and S. Fei (2011). "Validating satellite phenology through intensive ground observation and landscape scaling in a mixed seasonal forest." Remote Sensing of Environment **115**(1): 143-157.

Long, D. G. (2010). Standard BYU QuikSCAT and Seawinds Land/Ice Image Products. Provo, Microwave Earth Remote Sensing Laboratory, Brigham Young University.

Long, D. G., P. J. Hardin and P. T. Whiting (1993). "Resolution enhancement of spaceborne scatterometer data." Geoscience and Remote Sensing, IEEE Transactions on **31**(3): 700-715.

Mitchard, E. T. A., P. Meir, C. M. Ryan, E. Woollen, M. Williams, L. E. Goodman, J. A. Mucavele, P. Watts, I. H. Woodhouse and S. S. Saatchi (2012). "A novel application of satellite radar data: measuring carbon sequestration and detecting degradation in a community forestry project in Mozambique." Plant Ecology and Diversity **in press**.

Myers, B. A., R. J. Williams, I. Fordyce, G. A. Duff and D. Eamus (1998). "Does irrigation affect leaf phenology in deciduous and evergreen trees of the savannas of northern Australia?" Austral Ecology **23**(4): 329-339.

Nicholson, S. E. (2000). "The nature of rainfall variability over Africa on time scales of decades to millenia." Global and Planetary Change **26**(1-3): 137-158.

Olson, D. M., E. Dinerstein, E. D. Wikramanayake, N. D. Burgess, G. V. N. Powell, E. C. Underwood, J. A. D'Amico, I. Itoua, H. E. Strand, J. C. Morrison, C. J. Loucks, T. F. Allnutt, T. H. Ricketts, Y. Kura, J. F. Lamoreux, W. W. Wettengel, P. Hedao and K. R. Kassem (2001). "Terrestrial Ecoregions of the World: A New Map of Life on Earth." BioScience **51**(11): 933-938.

Reed, B. C., J. F. Brown, D. Vanderzee, T. R. Loveland, J. W. Merchant and D. O. Ohlen (1994). "Measuring Phenological Variability from Satellite Imagery." Journal of Vegetation Science **5**(5): 703-714.

Reich, P. B. (1995). "Phenology of tropical forests: patterns, causes, and consequences." Canadian Journal of Botany-Revue Canadienne De Botanique **73**(2): 164-174.

Ryan, C. M. (2009). Carbon Cycling, Fire and Phenology in a Tropical Savanna Woodland in Nhambita, Mozambique. School of Geosciences. Edinburgh, University of Edinburgh**:** 257.

Ryan, C. M., T. Hill, E. Woollen, C. Ghee, E. Mitchard, G. Cassells, J. Grace, I. H. Woodhouse and M. Williams (2012). "Quantifying small-scale deforestation and forest degradation in African woodlands using radar imagery." Global Change Biology **18**(1): 243-257.

Ryan, C. M. and M. Williams (2011). "How does fire intensity and frequency affect miombo woodland tree populations and biomass?" Ecological Applications **21**(1): 48-60.

Ryan, C. M., M. Williams and J. Grace (2011). "Above- and Belowground Carbon Stocks in a Miombo Woodland Landscape of Mozambique." Biotropica **43**(4): 423-432.

Schwartz, M. D. (2003). Phenology : an integrative environmental science. Dordrecht ; Boston, Kluwer Academic Publishers.

Schwartz, M. D. and J. M. Hanes (2010). "Intercomparing multiple measures of the onset of spring in eastern North America." International Journal of Climatology **30**(11): 1614-1626.

Simioni, G., J. Gignoux, X. Le Roux, R. Appe and D. Benest (2004). "Spatial and temporal variations in leaf area index, specific leaf area and leaf nitrogen of two co-occurring savanna tree species." Tree Physiol **24**(2): 205-216.

Singh, K. P. and C. P. Kushwaha (2005). "Emerging paradigms of tree phenology in dry tropics." Current Science **89**(6): 964-975.

Spencer, M. W., C. Wu and D. G. Long (2000). "Improved resolution backscatter measurements with the SeaWinds pencil-beam scatterometer." Geoscience and Remote Sensing, IEEE Transactions on **38**(1): 89-104.

Studer, S., R. Stockli, C. Appenzeller and P. L. Vidale (2007). "A comparative study of satellite and ground-based phenology." International Journal of Biometeorology **51**(5): 405-414.

Tinley, K. L. (1977). Framework of the Gorongosa Ecosystem. Faculty of Science. Pretoria, University of Pretoria**:** 184.

Tuohy, J. M. and J. S. Choinski (1990). "Comparative Photosynthesis in Developing Leaves of Brachystegia-Spiciformis Benth." Journal of Experimental Botany **41**(229): 919-923.

Ulaby, F. T., C. T. Allen, G. Eger Iii and E. Kanemasu (1984). "Relating the microwave backscattering coefficient to leaf area index." Remote Sensing of Environment **14**(1-3): 113-133.

Wagner, W., G. Lemoine, M. Borgeaud and H. Rott (1999). "A study of vegetation cover effects on ERS scatterometer data." Geoscience and Remote Sensing, IEEE Transactions on **37**(2): 938-948.

White, F. (1983). The vegetation of Africa : a descriptive memoir to accompany the Unesco/AETFAT/UNSO vegetation map of Africa. Paris, Unesco.

White, M. A., K. M. De Beurs, K. Didan, D. W. Inouye, A. D. Richardson, O. P. Jensen, J. O'Keefe, G. Zhang, R. R. Nemani, W. J. D. Van Leeuwen, J. F. Brown, A. De Wit, M. Schaepman, X. Lin, M. Dettinger, A. S. Bailey, J. Kimball, M. D. Schwartz, D. D. Baldocchi, J. T. Lee and W. K. Lauenroth (2009). "Intercomparison, interpretation, and assessment of spring phenology in North America estimated from remote sensing for 1982–2006." Global Change Biology **15**(10): 2335-2359.

Williams, R. J., B. A. Myers, W. J. Muller, G. A. Duff and D. Eamus (1997). "Leaf phenology of woody species in a North Australian tropical savanna." Ecology **78**(8): 2542-2558.

760 Woodhouse, I. H. and D. H. Hoekman (2000a). "Determining land-surface parameters from the ERS wind scatterometer." Geoscience and Remote Sensing, IEEE Transactions on **38**(1): 126-140.

Woodhouse, I. H. and D. H. Hoekman (2000b). "Determining Land-Surface Parameters from the ERS Wind Scatterometer." IEEE Transactions on Geoscience and Remote Sensing 38 (2000) 1.: 126-140.

Zhang, X., M. A. Friedl, C. B. Schaaf, A. H. Strahler, J. C. F. Hodges, F. Gao, B. C. Reed and A. Huete (2003). "Monitoring vegetation phenology using MODIS." Remote Sensing of Environment **84**: 471-475.